Supporting Information

Huang et al. 10.1073/pnas.0910749106

SI Methods

Histology and Immunohistochemistry. Protocols for standard histology (H&E), special stains, immunohistochemistry, and confocal microscopy are available at http://www.uphs.upenn.edu/mcrc/histology/histologyhome.html. For histological analyses of control and mutant hearts, 5- to 6-μm parasagittal sections were cut from paraffin-embedded hearts in the midline to expose all four cardiac chambers. Ten adjacent serial sections were inspected by two blinded observers and representative photomicrographs obtained. H&E staining and Masson's Trichrome staining were performed as described previously (1). Fibrosis was quantified in Masson's trichrome stained sections of the LV freewall and septum harvested from P300 αMyH*X-Cre*/*Myocd*$^{F/F}$-mutant ($n = 10$) and *Myocd*$^{F/F}$-control mice ($n = 10$) using NIH Image J software (1). Data are expressed as % fibrosis ± SEM. TUNEL staining of tamoxifen-treated *MerCreMer*/*Myocd*$^{F/F}$ and *Myocd*$^{F/F}$ hearts was performed as described (2). Quantification of TUNEL-staining was performed counting the number of cardiomyocytes/high-power field (HPF) and TUNEL-positive nuclei cardiomyocyte nuclei/HPF by a blinded observer in sections of LV tissue harvested from tamoxifen-treated *MerCreMer*/*Myocd*$^{F/F}$-mutant mice ($n = 6$) and tamoxifen-treated *Myocd*$^{F/F}$-control mice ($n = 6$). Sections were costained with MF20 antibody (1:100) (Developmental Hybridoma Bank) to identify cardiomyocytes. Twenty-five HPFs from sections showing the LV freewall and septum were counted per mouse. Data are expressed as the mean % apoptotic cardiomyocytes ± SEM.

For immunohistochemical analyses, these primary antibodies were used at the indicated dilution: rabbit polyclonal anti-mouse myocardin (1:125) (3), monoclonal anti-Cre (1: 500) (Sigma, clone 7–23), monoclonal anti-cardiac α-actin (1:10) (American Research Products, Ac1–20.4.2), monoclonal anti-MLC2v (1: 5) (AXXORA, ALX-BC-1150-S-L001), monoclonal anti-p53 (1:25) (Santa Cruz, clone sc-126), monoclonal anti-tropomyosin (1:100) (Sigma, clone TM311), monoclonal anti-α actinin (1:100) (Sigma, clone EA-53), monoclonal anti-desmin (1: 100) (DAKO, D33), polyclonal anti-Cx43 (1:50) (Zymed), monoclonal anti-N-Cadherin (1:200) (Zymed), monoclonal anti-β-catenin (1:100) (BD Transduction Labs Biosciences), polyclonal anti-cleaved caspase 3 (1:25) (Biocare, CP229A), monoclonal anti-caspase-9 (1:25) (Santa Cruz, sc-17784), and polyclonal anti-Bcl-$x_{S/L}$ (1:25) (Santa Cruz, sc-1690). Secondary antibodies used included: Alexa Fluor 488 goat anti-mouse IgG and rabbit anti-mouse IgG, Alexa Fluor 568 goat anti-rabbit IgG and rabbit anti-mouse IgG (Invitrogen), donkey anti-goat IgG, donkey anti-rabbit IgG, donkey anti-mouse IgG HRP (Jackson ImmunoResearch). Confocal microscopy was performed on a Leica PCS SP2 microscope as described previously (3).

Electron Microscopy. For electron microscopic analyses, hearts were perfused with relaxation solution (4), fixed in 2% glutaraldehyde with 0.1 M sodium cacodylate (pH 7.4) for 72 h at 4 °C. Electron microscopy was performed in the University of Pennsylvania EM Core Laboratory as described previously (3).

1. Xu J, et al. (2009) Cardiomyocyte-specific loss of neurofibromin promotes cardiac hypertrophy and dysfunction. *Circ Res* 105:304–311.
2. Gavrieli Y, Sherman Y, Ben-Sasson SA (1992) Identification of programmed cell death in situ via specific labeling of nuclear DNA fragmentation. *J Cell Biol* 119:493–501.
3. Huang J, et al. (2008) Myocardin regulates expression of contractile genes in smooth muscle cells and is required for closure of the ductus arteriosus in mice. *J Clin Invest* 118:515–525.
4. Jones WK, et al. (1996) Ablation of the murine alpha heavy chain gene leads to dosage effects and functional deficits in the heart. *J Clin Invest* 98:1906–1917.

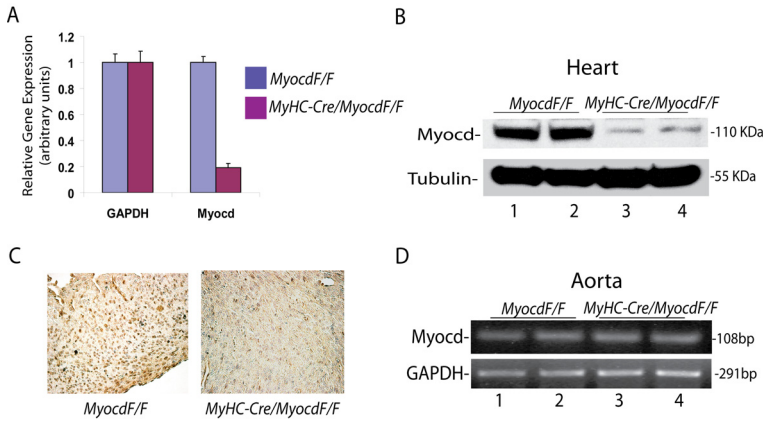

Fig. S1. Myocardin expression in hearts of *MyHC-Cre/Myocd*$^{F/F}$-mutant mice. (*A*) Myocardin gene expression in hearts of 3-month-old (P90) *MyHC-Cre/Myocd*$^{F/F}$-mutant mice ($n = 3$) and *Myocd*$^{F/F}$ ($n = 3$) controls. Real time qRT-PCR was performed to quantify myocardin mRNA in the hearts of P90 *MyHC-Cre/Myocd*$^{F/F}$-mutant (*red bars*) and control mice (*blue bars*). Data are expressed as mean gene expression (arbitrary units) ± SEM. (*B*) Western blot analyses was performed with cardiac protein lysates harvested from P300 *Myocd*$^{F/F}$ control ($n = 2$) and *MyHC-Cre/Myocd*$^{F/F}$-mutant ($n = 2$) mice. Densitometry performed with Image Quant 5.0 software revealed a 90% reduction in the 110-kDa band corresponding to myocardin (Myocd) protein in the *MyHC-Cre/Myocd*$^{F/F}$-mutant mice compared to controls. β-tubulin (Tubulin) is shown as the loading control. (*C*) Immunohistochemical analyses performed with rabbit polyclonal anti-myocardin antibody [Huang J, et al. (2008) Myocardin regulates expression of contractile genes in smooth muscle cells and is required for closure of the ductus arteriosus in mice. *J Clin Invest* 118(2):515–525.] demonstrated markedly diminished myocardin expression (*brown nuclear stain*) in cardiomyocytes of a P300 *MyHC-Cre/Myocd*$^{F/F}$-mutant mouse compared to a control *Myocd*$^{F/F}$ littermate. (*D*) qRT-PCR performed with mRNA harvested from the aorta of P300 *Myocd*$^{F/F}$-control ($n = 2$) and *MyHC-Cre/Myocd*$^{F/F}$-mutant ($n = 2$) mice revealed comparable levels of myocardin gene expression. A representative ethidium-stained agarose gel demonstrating the 108-bp myocardin and 291-bp GAPDH reaction products is shown.

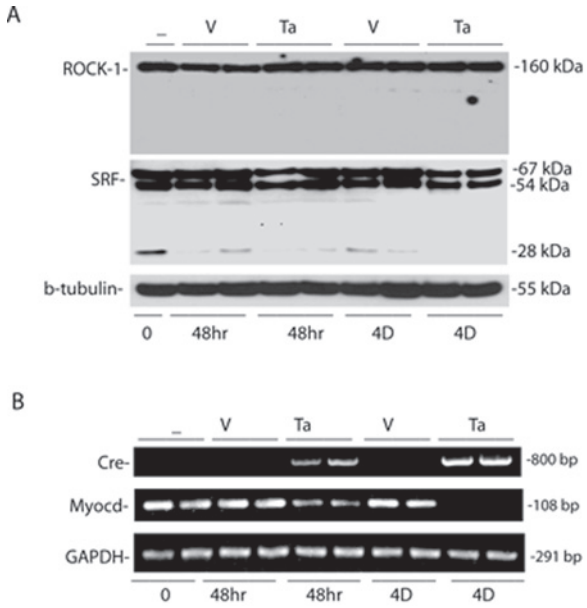

Fig. S2. Cardiomyopathy is not dependent upon caspase-3-mediated cleavage of SRF or ROCK-1. (*A*) Western blot analyses of SRF and ROCK1 protein in tamoxifen-treated *MerCreMer/Myocd*$^{F/F}$-conditional mutant mice. *MerCreMer/Myocd*$^{F/F}$-conditional mutant mice were treated with tamoxifen (Ta) or vehicle (V) control for 48 h and 96 h (4D) ($n = 2$ in each group) before being killed. Western blot analyses were performed with anti-SRF C-terminal antibody (G-20, Santa Cruz), anti-ROCK-1 antibody (G-6, Santa Cruz), and anti-β-tubulin antibody (ab6046, Abcam), as described previously [Huang J, et al. (2008) Myocardin regulates expression of contractile genes in smooth muscle cells and is required for closure of the ductus arteriosus in mice. *J Clin Invest* 118(2):515–525.]. MW markers are shown to the right of each blot. (*B*) qRT-PCR was performed with mRNA harvested from vehicle (V)- and tamoxifen (Ta)-treated *MerCreMer/Myocd*$^{F/F}$-conditional mutant mice as described previously by Huang et al. The panels show the ethidium-stained agarose gel containing reaction products harvested after 30 cycles corresponding to Cre recombinase (800-bp), myocardin (Myocd) (108-bp), and GAPDH (291-bp).

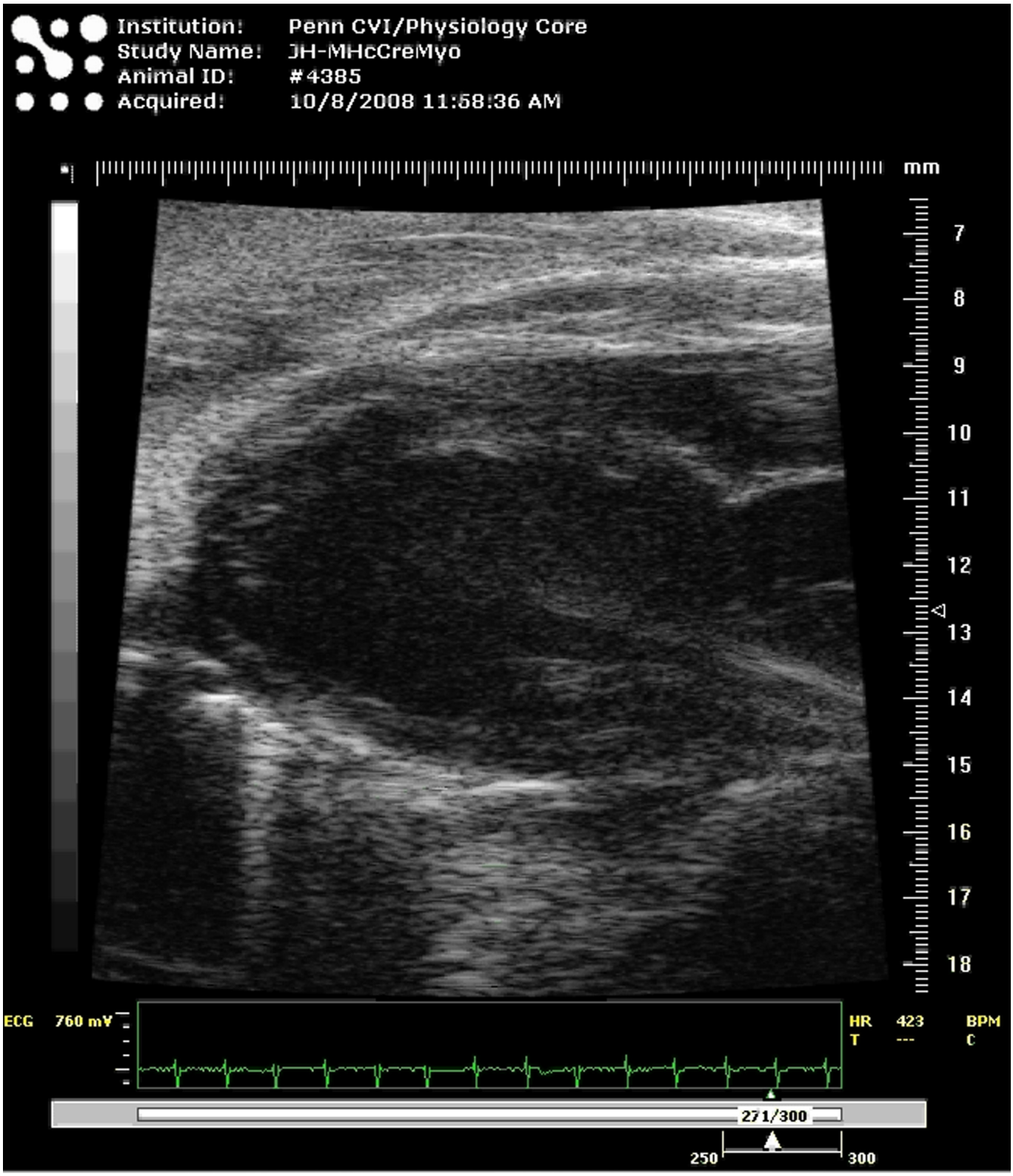

Movie S1. Two-dimensional echocardiogram long-axis view taken of a P300 *Myocd*$^{F/F}$-control mouse heart demonstrating normal LV dimensions and function. Scale in millimeters is shown above and to the right of the echocardiogram. ECG recording is shown below the echocardiogram. The frame rate has been slowed to 30 frames per second to facilitate visualization of cardiac contraction and relaxation.

Movie S1 (AVI)

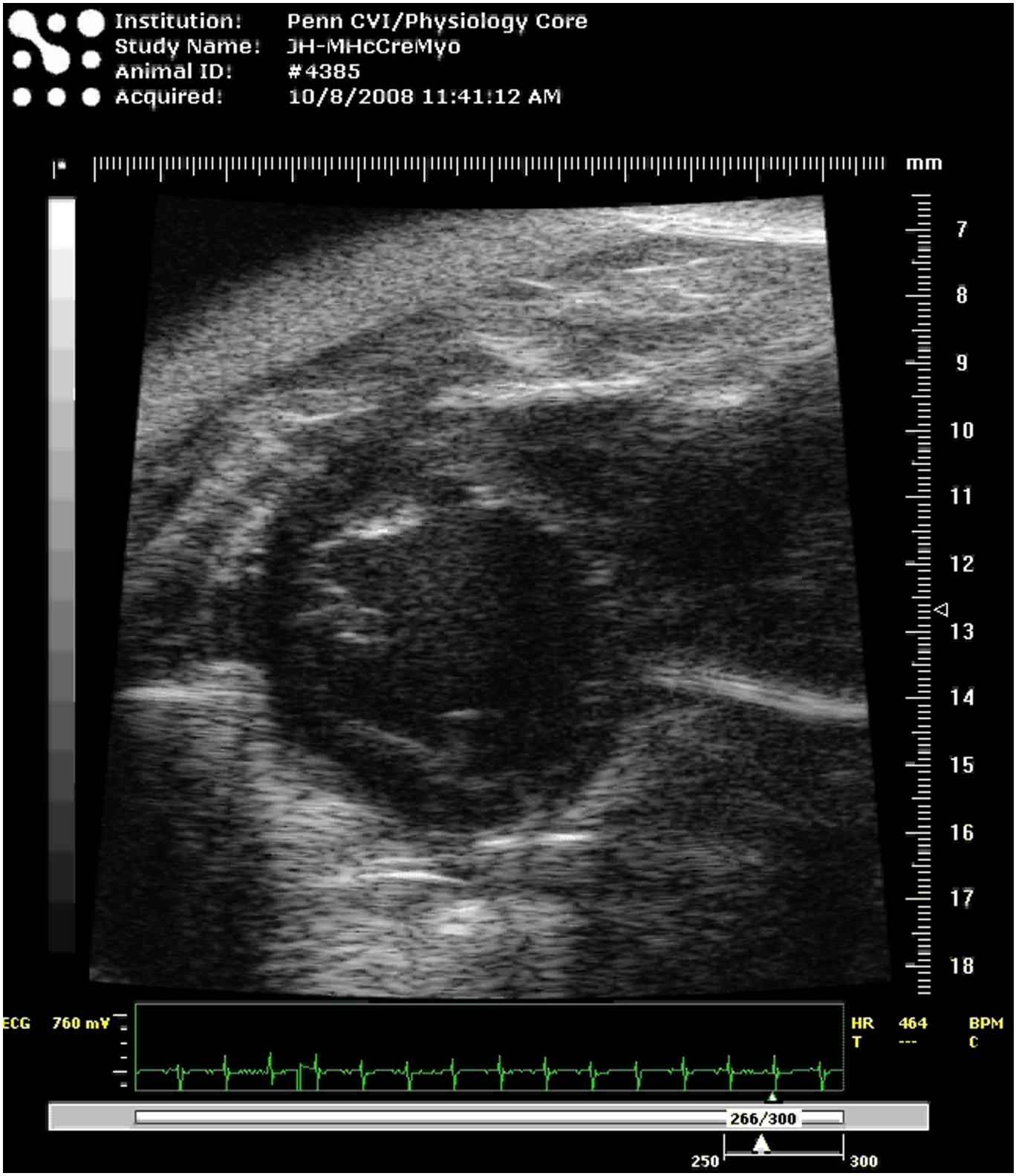

Movie S2. Two-dimensional echocardiogram short-axis view taken of a P300 *Myocd*$^{F/F}$-control mouse heart demonstrating normal LV dimensions and function.

Movie S2 (AVI)

Movie S3. Two-dimensional echocardiogram long-axis view taken of a P300 *MyHC-Cre/Myocd*$^{F/F}$-mutant mouse heart demonstrating dilated LV systolic and diastolic dimensions and globally decreased LV systolic function.

Movie S3 (AVI)

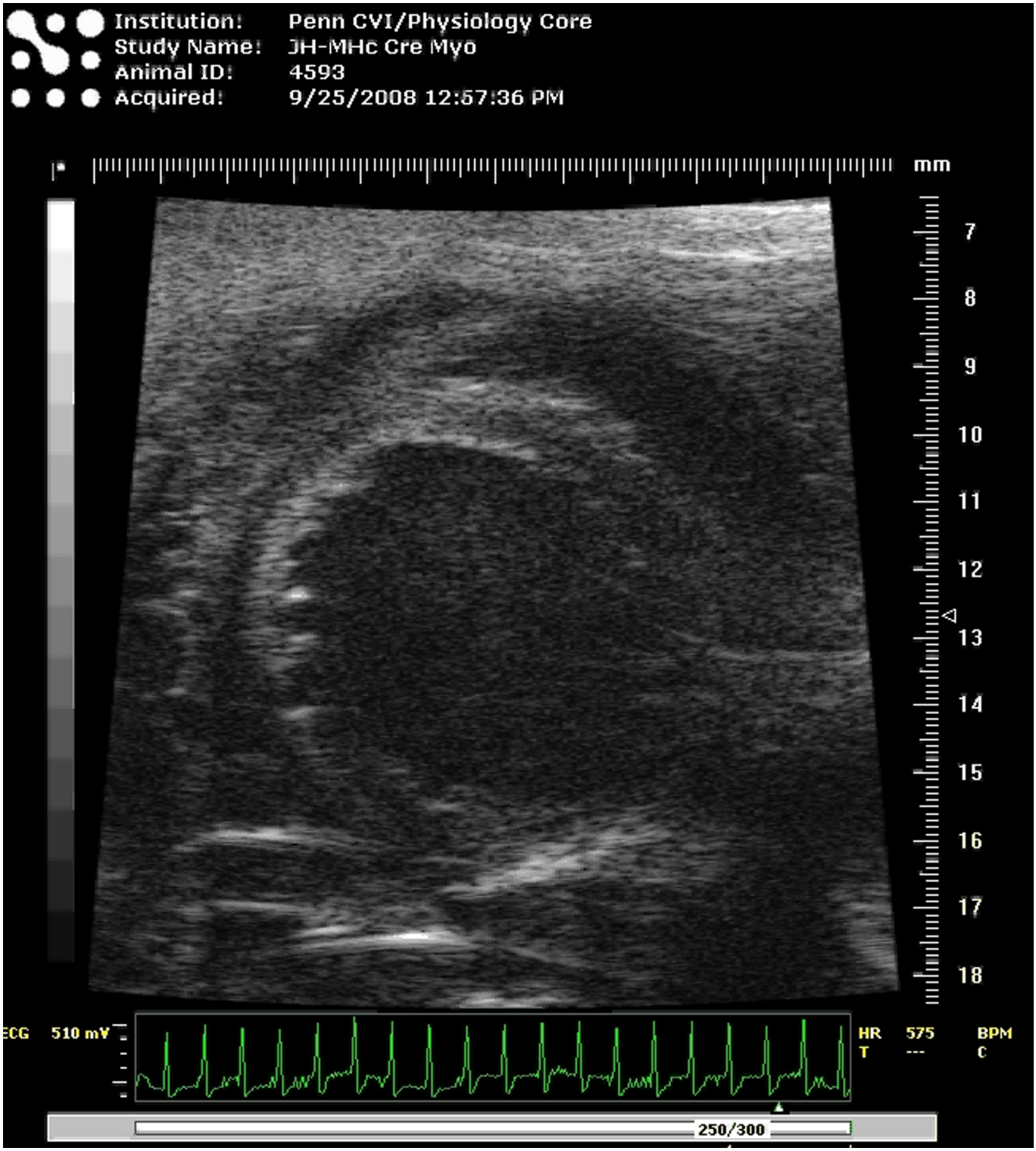

Movie S4. Two-dimensional echocardiogram short-axis view taken of a P300 *MyHC-Cre*/*Myocd*$^{F/F}$-mutant mouse heart demonstrating dilated LV systolic and diastolic dimensions and globally decreased LV systolic function.

Movie S4 (AVI)

Movie S5. Two-dimensional echocardiogram long-axis view taken 6-days following initiation of tamoxifen treatment of a *Myocd*$^{F/F}$-control mouse demonstrating normal LV dimensions and function.

Movie S5 (AVI)

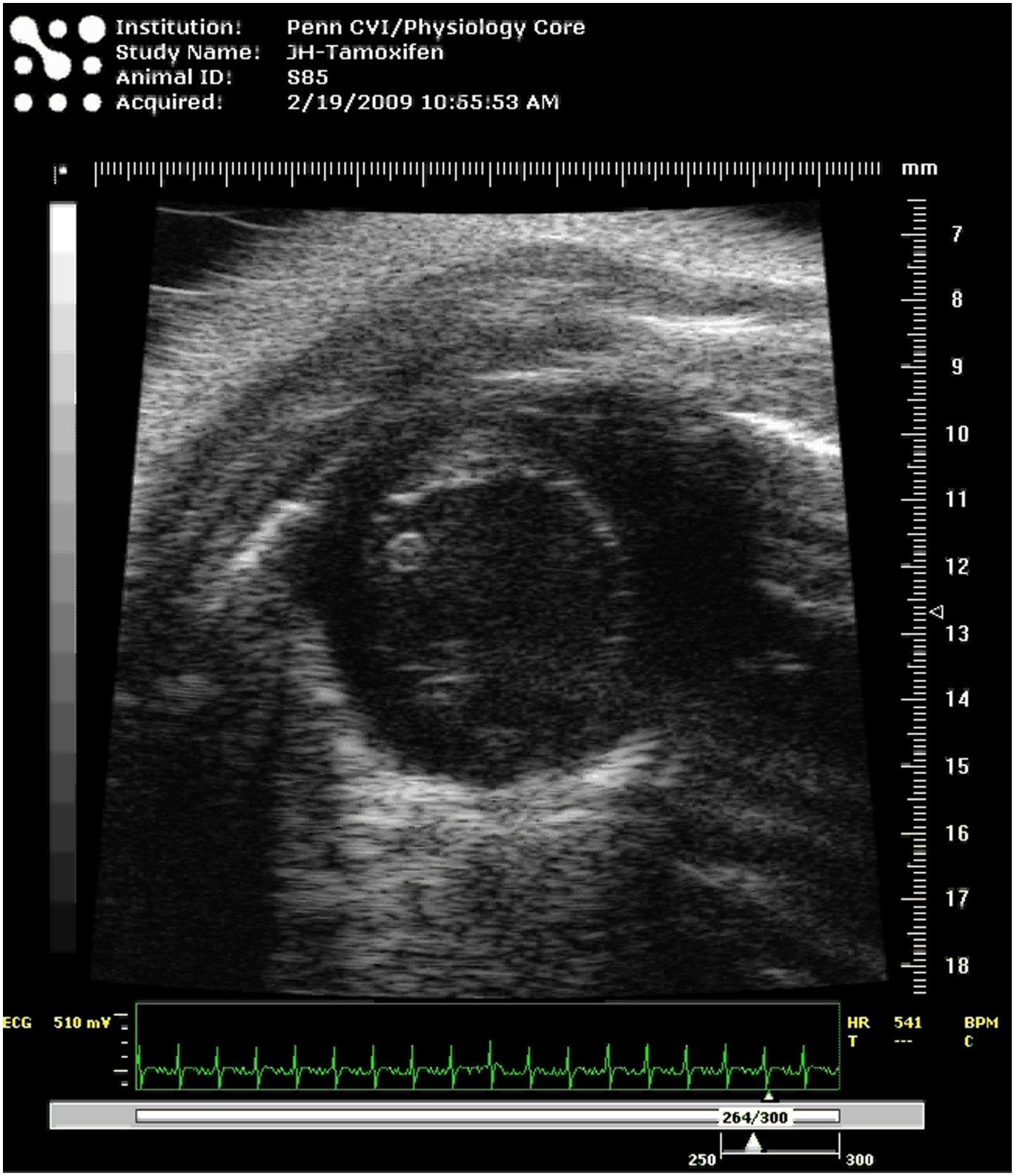

Movie S6. Two-dimensional echocardiogram short-axis view taken 6-days following initiation of tamoxifen treatment of a *Myocd*$^{F/F}$-control mouse demonstrating normal LV dimensions and function.

Movie S6 (AVI)

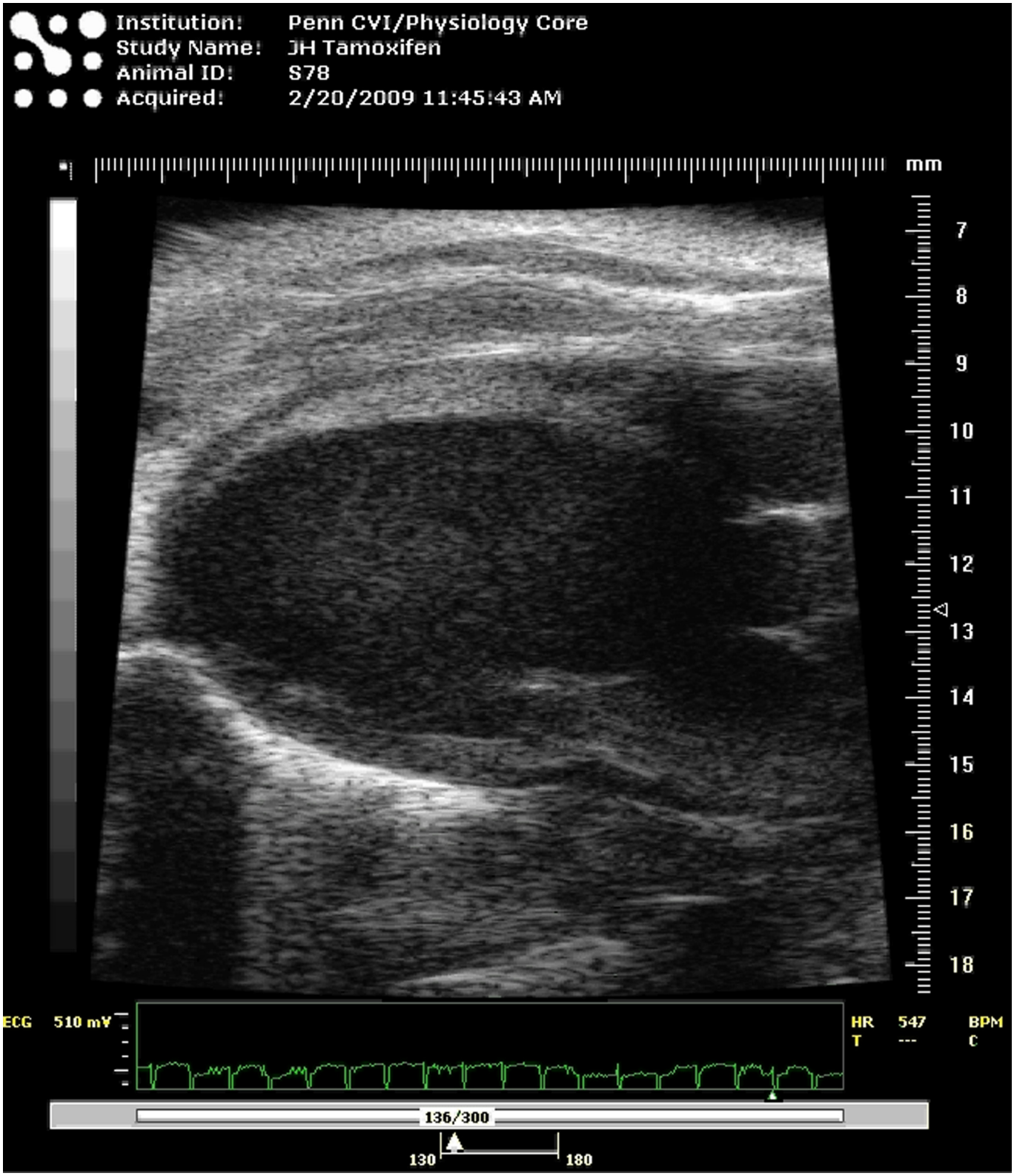

Movie S7. Two-dimensional echocardiogram long-axis view taken 6-days following initiation of tamoxifen treatment of a *MerCreMer/Myocd*$^{F/F}$ mouse demonstrating increased LV dimensions and globally reduced function.

Movie S7 (AVI)

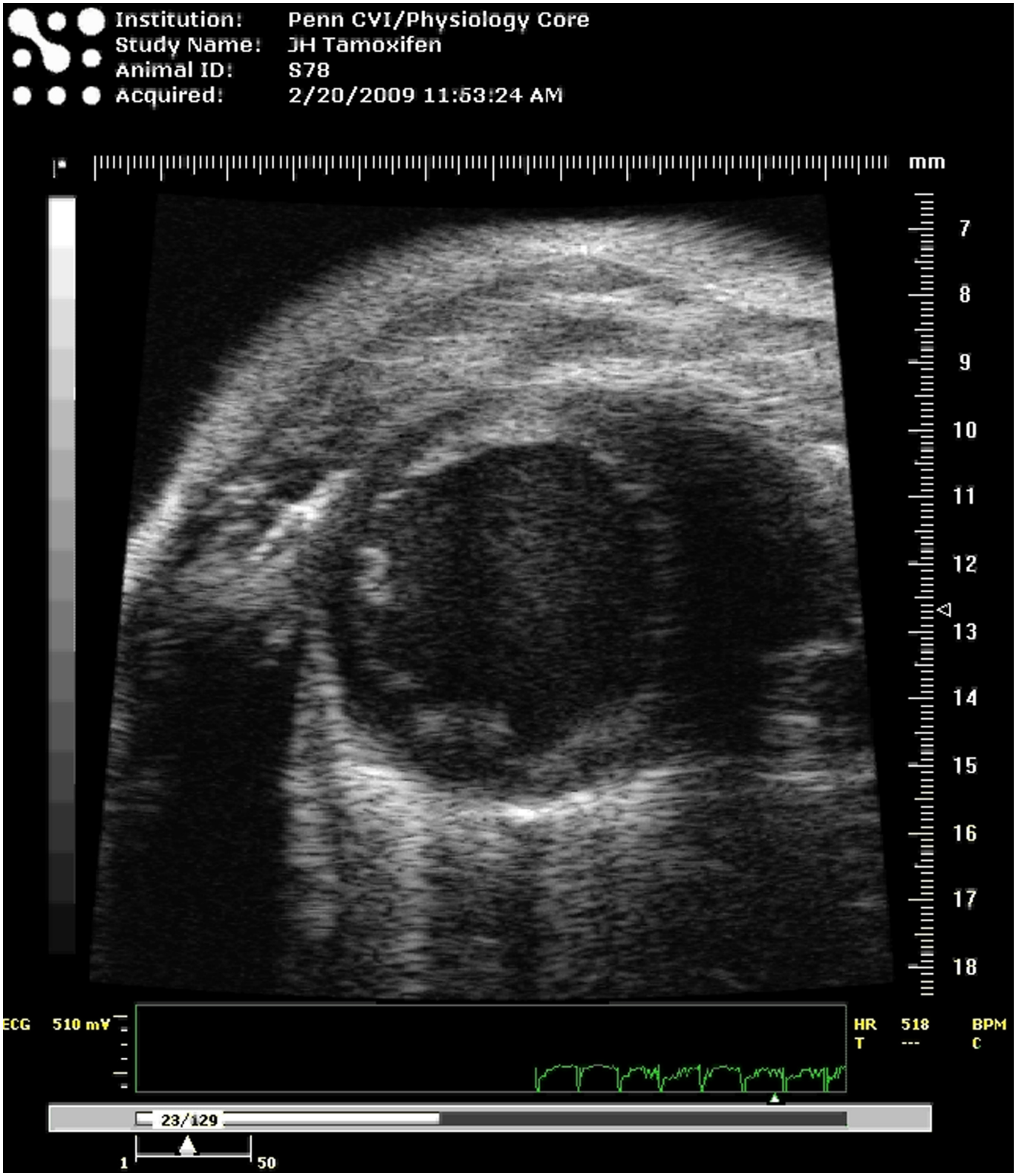

Movie S8. Two-dimensional echocardiogram short-axis view taken 6-days following initiation of tamoxifen treatment of a *MerCreMer/Myocd*$^{F/F}$ mouse demonstrating increased LV dimensions and globally reduced function.

Movie S8 (AVI)

Table S1. Morphometric and echocardiographic analyses of *MyH-Cre/Myocd*$^{F/F}$ mice

Measurement	*Myocd*$^{F/F}$ ($n = 10$)	*MyHC-Cre/Myocd*$^{F/F}$ ($n = 10$)	*P*
HW (mg)	187.3 ± 33.8	239.7 ± 101	0.14
BW (g)	37.7 ± 6.4	33.1 ± 6.5	0.13
HW/BW (mg/g)	5.1 ± 0.7	7.3 ± 3.1	<0.05[a]
IVSd (mm)	0.75 ± 0.10	0.63 ± 0.08	<0.01[a]
LVPWd (mm)	0.77 ± 0.07	0.62 ± 0.08	<0.001[a]
LVIDd (mm)	4.3 ± 0.3	5.4 ± 0.6	<0.0001[a]
LVIDs (mm)	3.0 ± 0.3	4.8 ± 0.6	<0.0001[a]
RV(A-P) (mm)	1.38 ± 0.33	1.97 ± 0.54	<0.05[a]
LA(area)(mm^2)	4.28 ± 0.77	8.14 ± 2.1	<0.0005[a]
RA(area)(mm^2)	3.82 ± 0.86	6.85 ± 2.1	<0.005[a]
EF (%)	57.8 ± 5.8	24.5 ± 7.3	<0.0001[a]
FS (%)	30.3 ± 3.8	11.5 ± 3.6	<0.0001[a]

[a]$P < 0.05$

BW, body weight; EF, ejection fraction; FS, fractional shortening; HW, heart weight; IVSd, interventricular septum dimension; LVPWd, left ventricular posterior wall dimension; LVIDd, left ventricular internal dimension in diastole; LVIDs, left ventricular internal dimension in systole; [RV(A-P)], left ventricular anterior to posterior diameter.

Table S2. Morphometric and echocardiographic analyses of *MerCreMer/Myocd*$^{F/F}$ mice

Measurement	*Myocd*$^{F/F}$ (+ tamoxifen) ($n = 6$)	*MerCreMerMyocd*$^{F/F}$ (pretreatment) ($n = 3$)	*MerCreMerMyocd*$^{F/F}$ (+ tamoxifen) ($n = 6$)	*P*
HW (mg)	138.0 ± 6.1	148.0 ± 5.5	162.3 ± 6.1	<0.05[a,b]
TL (mm)	18.1 ± 0.6	18.1 ± 0.4	18.0 ± 0.3	<0.01[a,b]
HW/TL (mg/mm)	7.6 ± 0.4	8.1 ± 0.5	9.0 ± 0.4	<0.01[a,b]
IVSd (mm)	0.72 ± 0.01	0.70 ± 0.07	0.77 ± 0.01	<0.05[a,b]
LVPWd (mm)	0.71 ± 0.01	0.71 ± 0.02	0.68 ± 0.09	<0.13
LVIDd (mm)	4.3 ± 0.1	4.05 ± 0.53	4.7 ± 0.2	<0.05[a,b]
LVIDs (mm)	3.0 ± 0.2	2.9 ± 0.3	4.4 ± 0.2	<0.001[a,b]
RV(A-P) (mm)	1.09 ± 0.18	1.18 ± 0.3	1.79 ± 0.46	<0.01[a,b]
LA(area)(mm^2)	5.33 ± 1.11	4.31 ± 1.22	8.18 ± 1.93	<0.01[a,b]
RA(area)(mm^2)	4.72 ± 1.0	3.58 ± 1.15	6.20 ± 1.35	<0.01[a,b]
EF (%)	58.7 ± 5.7	56.0 ± 4.9	14.9 ± 4.7	<0.001[a,b]
FS (%)	31.0 ± 3.9	33.1 ± 4.3	6.7 ± 2.2	<0.001[a,b]

[a]$P < 0.05$ versus *Myocd*$^{F/F}$

[b]$P < 0.05$ versus untreated *MerCreMer/Myocd*$^{F/F}$ *mice*

BW, body weight; EF, ejection fraction; FS, fractional shortening; HW, heart weight; IVSd, interventricular septum dimension; LVPWd, left ventricular posterior wall dimension; LVIDd, left ventricular internal dimension in diastole; LVIDs, left ventricular internal dimension in systole; [RV(A-P)], left ventricular anterior to posterior diameter.